Comparison Study of Dynamic Models for One-stage and Two-stage Anaerobic Digestion Processes ⋆

Ning Pan, * **Haoping Wang** * **Yang Tian*** * **Elena Chorukova** ** **Ivan Simeonov** ** **Nicolai Christov** ***

* *School of Automation, Nanjing Unversuty of Science and Technology, Nanjing, China (e-mail: tianyang@njust.edu.cn)*
** *The Stephan Angeloff Institute of Microbiology, Bulgarian Academy of Sciences, Acad G. Bonchev str., bl.26, Sofia 1113, Bulgaria*
*** *CRISTAL, Lille University*

Abstract: Compared to traditional one-stage anaerobic digestion processes (OSAD) with biomethane production, this paper focuses on the study of biogas yield of the two-stage anaerobic digestion processes (TSAD), which are able to produce simultaneously biohydrogen and biomethane from lignocellusic materials. The one-stage and two-stage systems for anaerobic digestion are obtained based on our previous papers. Additionally, the static characteristics and extremum points of both systems are also investigated. The tracking of maximum points is realized by fuzzy-PID controller. Simulation results suggest that in comparison to OSAD, the increase in biogas production of TSAD can reach to 75.18% by control action, which means TSAD is a better choice considering biogas production.

Keywords: Anaerobic digestion, One-stage, Two-stage, Mathematical modeling, Gas production

1. INTRODUCTION

With the consumption of fossil energy and the deterioration of the environment, the search for clean and renewable energy has become a key issue in the literature. Bioenergy, as a typical renewable energy, has gained wide attention increasingly used for biofuels, chemicals and power generation (Jose et al. (2018)). As one of the most important biomass energy utilization technologies, anaerobic digestion process (ADP) can convert organic waste into soluble organic substances and energy carrier such as hydrogen and methane (Nguyen et al. (2015)). Compared with other kind of biomass, lignocellulosic biomass has been considered as the ideal feedstock for dark fermentation and the preferred substrate for gas production (Phuttaro et al. (2019)), due to its wide sources, low price, short regeneration time, low-carbon environmental protection, rich varieties and high carbohydrate content.

The application of two-stage ADP (TSAD) for simultaneous hydrogen (H2) and methane (CH4) production (Xing and Zhao (2009)) has been proposed as a promising technology for better process performance and higher energy yields as compared to the traditional one-stage ADP (OSAD) (Pohland and Ghosh (1971)). In TSAD, relatively fast growing acidogens and H2-producing bacteria are developed in the first-stage hydrogenic bioreactor and are involved in the production of volatile fatty acides (VFA) and H2. On the other hand, the slow growing acetogens and methanogens are developed in the second-stage methanogenic bioreactor, in which the produced VFA are further converted to CH4 and CO2 (Xing and Zhao (2009)).

Since then, the comparison of the performances of OSAD and TSAD has been debated extensively, and advantages/drawbacks of both systems have been evaluated for pretreatment (Pakarinen et al. (2011)), volatile solids removal efficiency (Gioannis et al. (2017)), energy recovery (Schievano et al. (2012)) and biochemical processes (Tapia-Venegas et al. (2013)). It has been tested that the overall gas production is 8% - 43% higher for TSAD in the large majority of experimental conditions and never significantly lower (Schievano et al. (2014)). Different mathematical models for predicting biohydrogen and biomethane potentials have been developed (Monlau et al. (2012)). However, only few articles focus on the comparison of the models between OSAD and TSAD. The objective of this study is to compare OSAD and TSAD biohydrogen and biomethane yields on the base of appropriate mathematical models.

The paper is organized as follows. Mathematical modeling has been established under mesophilic conditions in Section 2, representing the OSAD and TSAD processes. The static characteristics and the performances in terms of H2 and CH4 production are also evaluated. Then, in Section 3 fuzzy PID controller has been applied to maximize the biogas production of OSAD and TSAD processes. Numerical results are presented and discussed in Section 4. Finally, concluding remarks are given in Section 5.

⋆ This work is partially supported by the Intergovernmental international science and technology innovation cooperation key project of National Key R&D Program of China (2021YFE0102700).

2. MODELING OF OSAD AND TSAD

There are a lot of dynamic mass-balance models describing ADP. It is necessary to choose appropriate models or objective functions for different goals.

2.1 Dynamic Model of OSAD

Generally, traditional ADP can be divided into four main stages (Denchev et al. (2016)) .

- hydrolysis of undissolved high-molecular weight compounds (proteins, sugars, fats) to soluble low-molecular weight compounds (monosugars, aminoacids, long chain fatty acids, glycerol).
- acidogenesis-biodegradation of low-molecular weight compounds from the previous stage to VFA (propionate, butirate, acetate etc.), hydrogen and carbon dioxide.
- transformation of VFA to acetate, hydrogen and carbon dioxide.
- methanogenesis mediated by acetoclastic methanogens (converting acetate to methane and carbon dioxide) and hydrogenotrophic methanogens (producing methane from hydrogen and carbon dioxide).

Although H2 is produced in OSAD as well but only CH4 is considered as final product because of two factors. On the one hand, it can be transformed in methane by the hydrogenotrophic bacteria in termophilic conditions. On the other hand, in mezophilic conditions one part of H2 is transformed in CH4 by the hydrogenotrophic bacteria and another part is present in the biogas (1-2 %), but it is very difficult to be measured online. On the basis of experimental investigations and according to the relatively simple three-stage biochemical scheme of ADP, the following fifth-order Barth-Hill nonlinear one-stage model with one control input (the dilution rate D) is further used for simulation purposes (Simeonov et al. (2011); Wang et al. (2013)):

$$\frac{dS_0}{dt} = -DS_0 - \beta X_1 S_0 + DY_p S_0^{in} \quad (1)$$

$$\frac{dX_1}{dt} = \mu_1 X_1 - DX_1 \quad (2)$$

$$\frac{dS_1}{dt} = -DS_1 + \beta X_1 S_0 - \frac{\mu_1 X_1}{Y_1} \quad (3)$$

$$\frac{dX_2}{dt} = \mu_2 X_2 - DX_2 \quad (4)$$

$$\frac{dS_2}{dt} = -DS_2 + Y_b \mu_1 X_1 - \frac{\mu_2 X_2}{Y_2} \quad (5)$$

$$Q = Y_g \mu_2 X_2 \quad (6)$$

with

$$\mu_1 = \frac{\mu_{1max} S_1}{k_{s1} + S_1}, \mu_2 = \frac{\mu_{2max} S_2}{k_{s2} + S_2} \quad (7)$$

In this above mass-balance model, equation (1) describes the hydrolysis process of the substrate $S_0, g/dm^3$, where the first term reflects the effluent flow rate of liquid, the second one reflects the hydrolysis of the diluted organics by acidogenic bacteria, and the third one represents the influent flow rate of liquid with concentration of the diluted organics $S_0^{in}, g/dm^3$. Equation (2) describes the growth and changes of the acidogenic bacteria (with concentration $X_1, g/dm^3$), consuming the appropriate substrate (with concentration $S_1, g/dm^3$). The mass balance for this substrate is described by equation (3), where the first term reflects the consumption by the acidogenic bacteria, the second term - formed as a result of the hydrolysis, the third one - the substrate $S_1, g/dm^3$, in the effluent flow rate of liquid. Equation (4) describes the growth and changes of the methane producing (methanogenic) bacteria (with concentration $X_2, g/dm^3$), consuming acetate (with concentration $S_2, g/dm^3$). The mass balance equation for acetate in equation (5) has three terms in the right side. The first one reflects the acetate formed as a result of the activity of acidogenic bacteria, the second one - the consumption of acetate by the methanogenic bacteria, and the third one - the acetate in the effluent liquid. Equation (6) represents the output flow rafe of biomethane. The relations (7) present the specific growth rate of the acidogenic bacteria μ_1, h^{-1} and the specific growth rate of the methanogenic bacteria μ_2, h^{-1}, both of Monod Type.

2.2 Dynamic Model of TSAD

The application of TSAD for simultaneous H2 and CH4 production has been proposed as a promising technology for better process performance and higher energy yields as compared to the traditional one-stage CH4 production process which has been discussed in the above section. In TSAD, relatively fast growing acidogens and H2 producing microorganisms are developed in the first-stage hydrogenic bioreactor (BR1 with working volume V1) and are involved in the production of acetate, propionate, butyrate (acidogenesis) and H2. On the other hand, the slow growing acetogens and methanogens are developed in the second-stage methanogenic bioreactor (BR2 with working volume V2) in which the produced propionate and butyrate are further converted to acetate (acetogenesis) and after that to CH4 and CO2 (methanogensis) (Borisov and Simeonov (2016)).

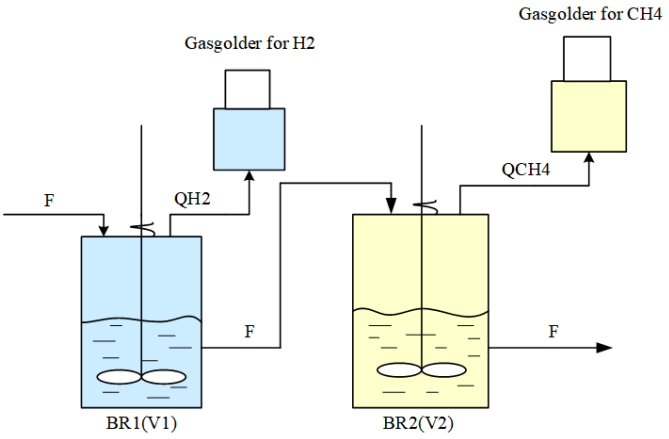

Fig. 1. TSAD with production of hydrogen and methane

Assume that the volumes V1 and V2 of the bioreactors are constant. Let F be the inflows in the first and second bioreactor. According to the scheme from Fig. 1, it is well known that the dilution rates in the first and second bioreactor D_1 and D_2 respectively are defined as:

$$D_1 = \frac{F}{V_1}, D_2 = \frac{F}{V_2} \quad (8)$$

With simple transformation it can be obtained:

$$K = \frac{V_2}{V_1} = \frac{D_1}{D_2} \tag{9}$$

A mass-balance model of continuous ADP for hydrogen production in BR1 presents a set of ODE and one algebraic equation as follows (Chorukova and Simeonov (2020)):

$$\frac{dPr_1}{dt} = \frac{\mu_1 X_1}{Y_{Pr1}} - D_1 Pr_1 \tag{10}$$

$$\frac{dBut_1}{dt} = \frac{\mu_1 X_1}{Y_{But1}} - D_1 But_1 \tag{11}$$

$$\frac{dAc_1}{dt} = \frac{\mu_1 X_1}{Y_{Ac1}} - D_1 Ac_1 \tag{12}$$

$$Q_{H_2} = Y_{H_2} \mu_1 X_1 \tag{13}$$

The balance of effluent substrate $S_0, g/dm^3$, cellulose concentration $S_1, g/dm^3$ and biomass concentration $X_1, g/dm^3$ is the same expression like Equation (1-3). Equation (10-12) reflect dynamics of the intermediate products formation - propionate $Pr_1, g/dm^3$ and butyrate $But_1, g/dm^3$, acetate $Ac_1, g/dm^3$. Equation (13) describes the flow rate of the hydrogen in the gas phase in BR1. The expression of specific growth rate of the biomass is a Monod type function as μ_1, h^{-1} in relation (7).

A balance model of the second stage of the process (methane production in the BR2 on the base of the acetate, propionate and butyrate produced in the BR1) is adopted consisting of a set of the following equations:

$$\frac{dX_{Pr}}{dt} = \mu_{Pr} X_{Pr} - D_2 X_{Pr} \tag{14}$$

$$\frac{dPr_2}{dt} = \frac{\mu_{Pr} X_{Pr}}{Y_{Pr2}} + D_2(Pr_1 - Pr_2) \tag{15}$$

$$\frac{dX_{But}}{dt} = \mu_{But} X_{But} - D_2 X_{But} \tag{16}$$

$$\frac{dBut_2}{dt} = \frac{\mu_{But} X_{But}}{Y_{Pr2}} + D_2(But_1 - But_2) \tag{17}$$

$$\frac{dX_{Ac}}{dt} = \mu_{Ac} X_{Ac} - D_2 X_{Ac} \tag{18}$$

$$\frac{dAc_2}{dt} = -\frac{\mu_{Ac} X_{Ac}}{Y_{Ac2}} + \frac{\mu_{Pr} X_{Pr}}{Y_{Pr2}} + \frac{\mu_{But} X_{But}}{Y_{Pr2}} + D_2(Ac_1 - Ac_2) \tag{19}$$

$$Q_{CH_4} = Y_{CH_4} \mu_{Ac} X_{Ac} \tag{20}$$

with

$$\mu_{Pr} = \frac{\mu_{Prmax} Pr_2}{k_{sPr} + Pr_2} \tag{21}$$

$$\mu_{But} = \frac{\mu_{Butmax} But_2}{k_{sBut} + But_2} \tag{22}$$

$$\mu_{Ac} = \frac{\mu_{Acmax} Ac_2}{k_{sAc} + Ac_2} \tag{23}$$

Equation (14) describes the dynamics of the propionate degrading population with concentration $X_{Pr}, g/dm^3$, equation (16) - the dynamics of thebutyrate degrading population with concentration $X_{But}, g/dm^3$, euqation (18) - the dynamics of the methanogenic population $X_{Ac}, g/dm^3$. Equations (15), (17) and (19) present the balances of the corresponding substrates (propionate, butyrate and acetate) with the concentrations (Pr_2, But_2 and $Ac_2, g/dm^3$). The equation (23) reflects the flow rate of the methane in the gas phase of BR2. The specific growth rates of all populations are described as Monod type functions (21-23). All the parameters are given in Table 1. (Wang et al. (2014))

2.3 Static Characteristics for OSAD

The simplest solutions of the model will be calculated in this part, namely equilibrium points. Transforming the differential equations of the balance models, some algebraic equations called static characteristics of both bioreactors were obtained. They represent dependencies of the main process variables from the dilution rates. On the basis of this results, the maximum value of of the corresponding biogas yields can be found.

The equilibrium points of OSAD are solutions of the algebraic equations obtained from equations (1-5) by setting the right-hand sides equal to zero (Borisov and Simeonov (2020)). The equilibrium points are computed as functions of the dilution rates D and inlet organics concentration S_0^{in}.

The specific growth rates μ_1, μ_2 satisfy the equation: $\mu_1 = \mu_2 = D$, that is, the equilibrium component $\bar{S}_1 = \bar{S}_1(D), \bar{S}_2 = \bar{S}_2(D)$ with respect to the phase variable S_0, S_1, are quivalent to the following formula:

$$\bar{S}_1(D) = \frac{k_{s1} D}{\mu_{1max} - D}, \bar{S}_2(D) = \frac{k_{s2} D}{\mu_{2max} - D}, \tag{24}$$

Furthermore, equilibrium components $\bar{S}_0, \bar{X}_1, \bar{S}_0, \bar{X}_2, \bar{Q}$ respectively, which is transforming by using Symbolyc toolbox of Matlab:

Table 1. Model parameters

	Definition of the model parameters	value
β	coefficient of biodegradability (-)	1
Y_p	coefficient (-)	2
Y_b	coefficient (-)	40
Y_g	coefficient (-)	1
Y_1	coefficient for acidogenic bacteria(-)	0.006(one-) 0.08(two-)
Y_2	coefficient for acidogenic bacteria(-)	1.1
μ_{1max}	maximum specific growth rate of acidogenic bacteria(h^{-1})	0.568
μ_{2max}	maximum specific growth rate of (h^{-1})	0.4
k_{s1}	saturation coefficient of acidogenic bacteria(g/dm^3)	3.914
k_{s2}	saturation coefficient of (g/dm^3)	1.9
Y_{Pr1}	yield coefficient for propionate(-)	4.2
Y_{But1}	yield coefficient for butyrate(-)	2.1
Y_{Ac1}	yield coefficient for acetate(-)	1.1
Y_{H_2}	yield coefficient for hydrogen(dm^3/g)	1
Y_{Pr2}	yield coefficient for propionate(-)	1.5
Y_{But2}	yield coefficient for butrate(-)	1.5
Y_{Ac2}	yield coefficient for acetate(-)	0.5
Y_{CH4}	yield coefficient for methane(dm^3/g)	142
μ_{Prmax}	maximum specific growth rate of propionate degarding bacteria(h^{-1})	0.05
k_{sPr}	saturation coefficient of propionate (g/dm^3)	0.22
μ_{Butmax}	maximum specific growth rate of butyrate degarding bacteria(h^{-1})	0.05
k_{sBut}	saturation coefficient of butyrate (g/dm^3)	0.22
μ_{Acmax}	maximum specific growth rate of methanogenic bacteria(h^{-1})	0.025
k_{sAc}	saturation coefficient of acetate (g/dm^3)	0.8

$$\bar{S}_0(D, S_0^{in}) = \frac{Y_p S_0^{in}}{\beta(P_1 - P_2)} \tag{25}$$

$$\bar{X}_1(D, S_0^{in}) = P_1 + P_2 \tag{26}$$

$$\bar{X}_2(D, S_0^{in}) = \frac{Y_b(P_1 + P_2) - \bar{S}_2(D)}{k_2} \tag{27}$$

$$\bar{Q}(D, S_0^{in}) = Y_g \bar{X}_2(D, S_0^{in}) D \tag{28}$$

$$P_1 = \frac{\mu_{1max} Y_1 Y_p S_0^{in} - k_{s1} Y_1 D - Y_1 Y_p S_0^{in} D}{2(\mu_{1max} - D)} \tag{29}$$

$$P_2 = \frac{D^2 - \mu_{1max} D + \sqrt{P_3}}{2\beta(\mu_{1max} - D)} \tag{30}$$

$$\begin{aligned} P_3 = {} & D^4 + 2\beta k_{s1} Y_1 D^3 - 2\beta Y_1 Y_p S_0^{in} D^3 - 2\mu_{1max} D^3 \\ & + \beta^2 k_{s1}^2 Y_1^2 D^2 + 2\beta^2 k_{s1}^2 Y_1^2 S_0^{in} D^2 - 2\beta k_{s1} Y_1 \mu_{1max} D^2 \\ & + \beta^2 Y_1^2 Y p^2 S_0^{in2} D^2 + 4\beta Y_1 Y_p \mu_{1max} S_0^{in} D^2 + \mu_{1max}^2 D^2 \\ & - 2\beta^2 k_{s1} Y_1^2 Y_p^2 S_0^{in} D - 2\beta^2 Y_1^2 Y_p^2 \mu_{1max} S_0^{in2} D \\ & - 2\beta Y_1 Y_p \mu_{1max}^2 S_0^{in} D + \beta^2 Y_1^2 Y_p^2 \mu_{1max}^2 S_0^{in2} \end{aligned} \tag{31}$$

By determining the possible steady states for given values of constant D, an input/output steady-state map $(\tilde{D}, \tilde{Q})$ can be built, considering the methane flow rate. There is the unique point (D_{max}, Q_{max}) with the derivative of Equation (28) where the biogas production rate is maximal. From the figures it can be seen that the maximum point is unique.

2.4 Static Characteristics for TSAD

In the same way the equilibrium points of TSAD can be calculated, which are solutions of the algebraic equations $\bar{S}_0, \bar{S}_1, \bar{X}_1, \bar{Pr}_1, \bar{But}_1, \bar{Ac}_1, \bar{Pr}_2, \bar{X_{Pr}}, \bar{But}_2, \bar{X_{But}}, \bar{Ac}_2, \bar{X_{Ac}}$ and $\bar{Q}_{H_2}, \bar{Q}_{CH_4}, \bar{Q}_{sum}$. The volume ratio K are considered as the constant when analizing the static characteristics. More details are shown in Chorukova and Simeonov (2020).

3. FUZZY-PID CONTROLLER DESIGN OF ADP

In this section a fuzzy-PID controller for biogas production is designed to ensure output trajectory tracking for both the nonlinear OSAD and TSAD.

With regard to optimal anaerobic treatment, fuzzy-logic controller permits dealing with uncertainties and does not require a rigorous mathematical model, so it is an interesting alternative especially in ADP which have nonlinear characteristics. Owing to lack of integral action, the fuzzy controller has poor performance for eliminating steady state error of the system, and high control precision is difficult to be achieved. However, with the integral regulation effect, classical PID controller can theoretically control the steady state error of the system to be zero, thus achieving better function on eliminating steady error.

Choosing the dilution rate as control input, the output of the fuzzy-PID controller is defined as

$$u = s(e)u_{FZ} + (1 - s(e))u_{PID} \tag{32}$$

The swithcing signal $s(e)$ is set as the function of the error $e = y_{ref} - y$:

$$s(e) = \begin{cases} 0 & |e| < E \\ 1 & |e| \geq E \end{cases} \tag{33}$$

The structure of fuzzy-PID controller is shown in the

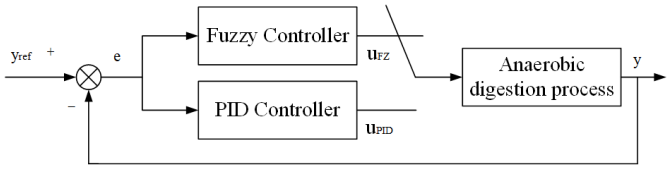

Fig. 2. Block diagram of fuzzy-PID control system

Fig. 2 which can integrate both advantages of two kinds of controllers.When an error is larger than the threshold E, fuzzy control is adopted to achieve better transient performance, otherwise, PID control is employed to obtain better steady state performance. It has good application in pH control and temperature control (Kang et al. (2009)) . By combining the advantages of fuzzy control and PID control, fuzzy PID control determines the controlled variable according to control rules and on-line detection results instead of a precise mathematical model.

4. NUMERICAL RESULTS

Numerical experiments using Simulink are performed in this section.With the aim of achieving the greatest gas production, the simulation results will be compared by using time responses to the step signal and comparing their tracking trajectory of the theoretical maximum point in static characteristic within the fuzzy-PID controller.

4.1 Open-loop Performance

Numerical experiments using Simulink of Matlab are performed for step changes of the dilution rates (presented in Table 2. Inlet cellulose concentration and the volumn ratio take value for $K = 26.5, S_0^{in} = 40 g/dm^3$. The dynamics of biogas rates are presented on Figs.3. Initial values of state variables are shown in Table 3. and Table 4. respectively.

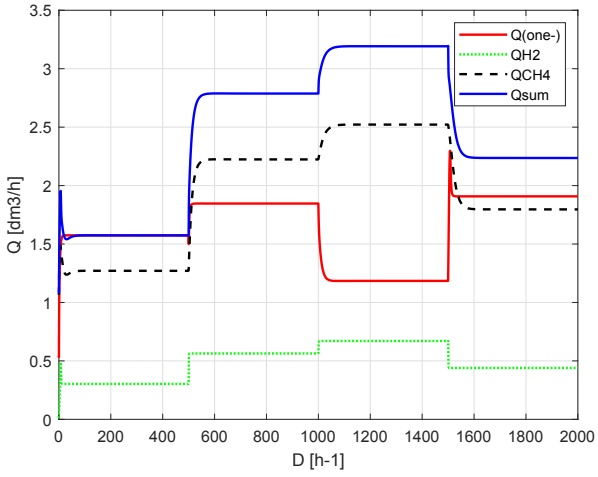

Fig. 3. The biogas flow rate in OSAD and TSAD.

Table 2. Step changes of the dilution rates

Time [h]	0-500	500-1000	1000-1500	1500-2000
$D[h^{-1}]$	0.1000	0.2000	0.2500	0.1500
$D_1[h^{-1}]$	0.1000	0.2000	0.2500	0.1500
$D_2[h^{-1}]$	0.0038	0.0075	0.0094	0.0057

It can be found that the total gas production in TSAD keeps increasing in comparison of OSAD with an increase in the dilution rate. However, the biogas flow rate does not always increase when the dilution rate increases. Hence it is more significant to find the limitation of the reactors from the static characteristics.

4.2 Static Characteristics and Maximum Points

The static characteristics of gas flow rate with dilution rate for different values of S_0^{in} in OSAD and TSAD are presented on Fig.4-6. The maximum points of the static characteristics are shown in Table 5.

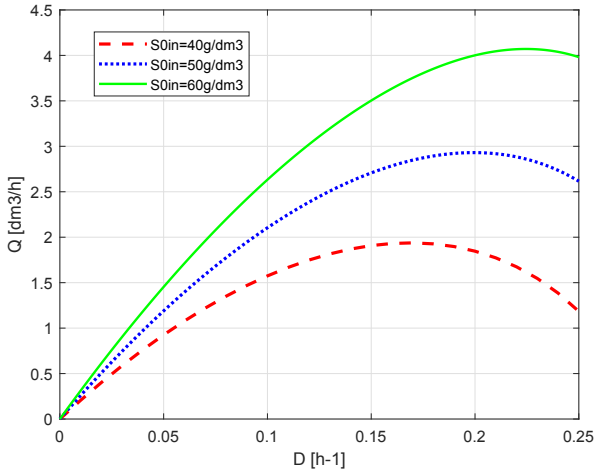

Fig. 4. Characteristic $Q(D)$ for different values of S_0^{in} in OSAD.

It has been presented that the maximum gas point in TSAD increases 55.8%-75.4% more than OSAD which has been shown in Table 5. Obviously, TSAD is much better than OSAD from the perspective of gas production. It is noteworthy that TSAD is slower time-varying process

Table 3. Initial value of variables in OSAD

variable	value
$S_0(0)$	10 g/dm^3
$S_1(0)$	0.18 g/dm^3
$X_1(0)$	0.36 g/dm^3
$X_2(0)$	15.66 g/dm^3
$S_2(0)$	0.18 g/dm^3

Table 4. Initial value of variables in TSAD

variable	value	variable	value
$S_0(0)$	10 g/dm^3	$Pr_2(0)$	0.1 g/dm^3
$S_1(0)$	0.18 g/dm^3	$But_2(0)$	0.1 g/dm^3
$X_1(0)$	0.36 g/dm^3	$Ac_2(0)$	0.1 g/dm^3
$Pr_1(0)$	0.5 g/dm^3	$X_{Pr}(0)$	1.2 g/dm^3
$But_1(0)$	0.5 g/dm^3	$X_{But}(0)$	2.4 g/dm^3
$Ac_1(0)$	0.5 g/dm^3	$X_{Ac}(0)$	2.7 g/dm^3

Table 5. Maximum value

Gas$[dm^3/h]$	$S_0^{in}=40$	$S_0^{in}=50$	$S_0^{in}=60$
Q(one-)	1.9379	2.9307	4.0707
Q_{H_2}(two-)	0.7956	1.1041	1.4288
Q_{CH_4}(two-)	2.6421	3.7573	4.9636
Q_{sum}(two-)	3.3996	4.8166	6.3430

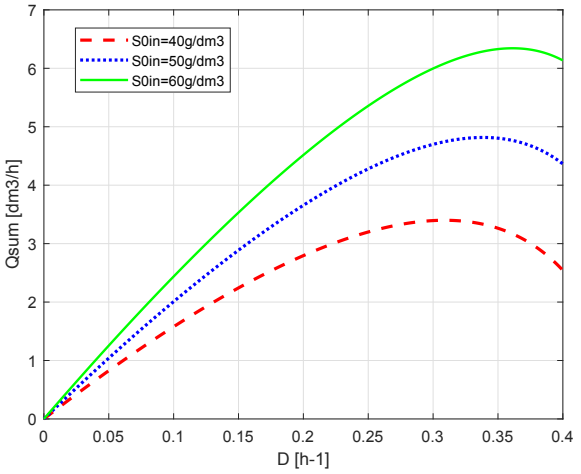

Fig. 5. Characteristic $Qsum(D) = Q_{H_2} + Q_{CH_4}$ for different values of S_0^{in} in TSAD.

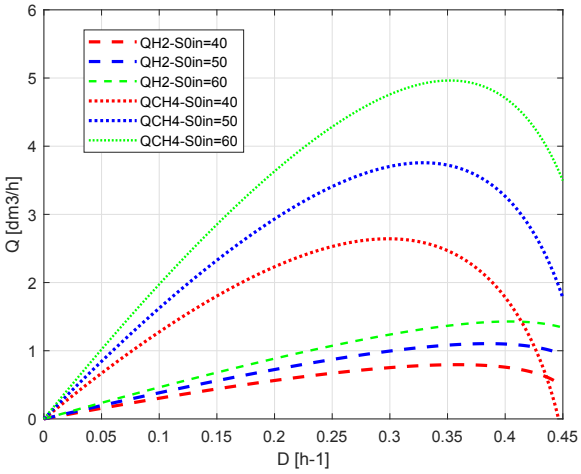

Fig. 6. Characteristic $Q_{H_2}(D)$ for different values of S_0^{in} in TSAD.

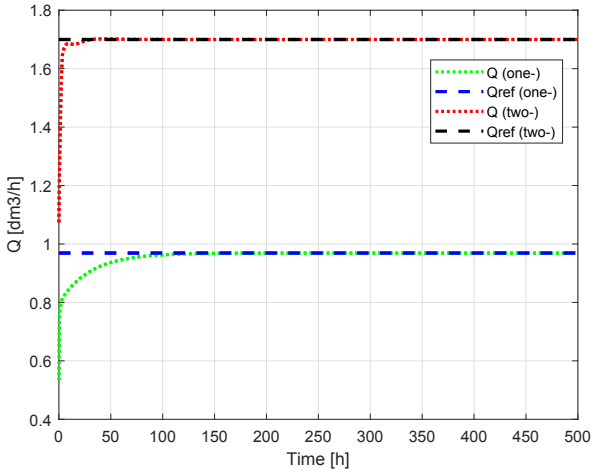

Fig. 7. Biogas flow rate within fuzzy-PID control in OSAD and TSAD.

comparing with the OSAD, which means lower sensitivities to the dilution rate.

4.3 Performance of fuzzy-PID Controller

In order to simulate ADP in laboratory conditions, fuzzy-PID controller has been added in the anaerobic digestion system. Measure white Gaussian noise in S_0^{in} is added. To avoid the situation of wash-out of microorganisms, fuzzy-PID controller is applicable only in the left-hand of the maximum for the biogas production. From the actual experience, the working point is chosen to be 50% of the maximum biogas production in table 5 as the tracking value. Therefore, the output trajectory for fuzzy-PID control are shown in Fig.7.

It can be seen that the output tracjectory by using fuzzy-PID controller has nearly no error within a relatively fast time response. Results show that adopting the two-stage system results in 75.19% comparatively higher total biogas production.

5. CONCLUSION

In this paper, one-stage and two-stage mathematical models of ADP have been compared in order to increase biogas production. Both models are proposed under the similiar assumption of the anaerobic biodegradation. The investigation of the equilibrum points and static characteristics shows the existence of maxima with respect to biogas yields. This fact is important for the practical applications and will be further used in optimising the bioreactors to achieve maximal production of either hydrogen and methane, which is a good possibility for realization of extremum-seeking control algorithms. According to the simulation results, the total gas in TSAD is higher (36.12%-169.59%) than OSAD in the same input condition. Furthermore, 75% increase of the maximum biogas flow rate achieves in the TSAD by fuzzy-PID controller, which implies better potentialities of biogas production.

Future work will develop more suitable control strategies to achieve maximal gas production that contribute to designing and engineering a real process.

REFERENCES

Borisov, M. Dimitrova, N. and Simeonov, I. (2016). Mathematical modelling of anaerobic digestion with hydrogen and methane production. *IFAC-PapersOnLine*.

Borisov, M. Dimitrova, N. and Simeonov, I. (2020). Mathematical modeling and stability analysis of a two-phase biosystem. *Chemical Engineering Journal*, 8(7), 791.

Chorukova, E. and Simeonov, I. (2020). Mathematical modeling of the anaerobic digestion in two-stage system with production of hydrogen and methane including three intermediate products - sciencedirect. *International Journal of Hydrogen Energy*, 45(20), 11550–11558.

Denchev, D., Hubenov, V., Simeonov, I., and Kabaivanova, L. (2016). Biohydrogen production from lignocellulosic waste with anaerobic bacteria. In *The 4th International Conference on Water, Energy and Environment*.

Gioannis, G.D., Muntoni, A., Polettini, A., Pomi, R., and Spiga, D. (2017). Energy recovery from one- and two-stage anaerobic digestion of food waste. *Waste Management*, 68(oct.), 595–602.

Jose, S., Bhaskar, T., Jose, S., and Bhaskar, T. (2018). *Biomass and Biofuels: Advanced Biorefineries for Sustainable Production and Distribution*. Biomass and Biofuels: Advanced Biorefineries for Sustainable Production and Distribution.

Kang, J., Wang, M., Xiao, Z., and Yan, Z. (2009). Fuzzy pid control of the ph in an anaerobic wastewater treatment process. In *International Workshop on Intelligent Systems and Applications*.

Monlau, F., Sambusiti, C., Barakat, A., Xin, M.G., Latrille, E., Trebly, E., Steyer, J.P., and Carrere, H. (2012). Predictive models of biohydrogen and biomethane production based on the compositional and structural features of lignocellulosic materials. *Environmental Science & Technology*, 46(21), 12217.

Nguyen, D., Gadhamshetty, V., Nitayavardhana, S., and Khanal, S.K. (2015). Automatic process control in anaerobic digestion technology: A critical review. *Bioresource Technology*.

Pakarinen, O.M., Kaparaju, P., and Rintala, J.A. (2011). Hydrogen and methane yields of untreated, water-extracted and acid (hcl) treated maize in one- and two-stage batch assays. *International Journal of Hydrogen Energy*, 36(22), 14401–14407.

Phuttaro, C., Sawatdeenarunat, C., Surendra, K.C., Boonsawang, P., ChaiPrApat, S., and Khanal, S.K. (2019). Anaerobic digestion of hydrothermally-pretreated lignocellulosic biomass: Influence of pretreatment temperatures, inhibitors and soluble organics on methane yield. *Bioresource Technology*, 284, 128–138.

Pohland, F.G. and Ghosh, S. (1971). Developments in anaerobic stabilization of organic wastes - the two-phase concept. *Envir Letters*, 1(4), 255–266.

Schievano, A., Tenca, A., Lonati, S., Manzini, E., and Adani, F. (2014). Can two-stage instead of one-stage anaerobic digestion really increase energy recovery from biomass? *Applied Energy*, 124(jul.1), 335–342.

Schievano, A., Tenca, A., Scaglia, B., Merlino, G., Rizzi, A., Daffonchio, D., Oberti, R., and Adani, F. (2012). Two-stage vs single-stage thermophilic anaerobic digestion: Comparison of energy production and biodegradation efficiencies. *Environmental Science & Technology*, 46(15), 8502–10.

Simeonov, I.S., Kalchev, B.L., and Christov, N.D. (2011). Parameter and state estimation of an anaerobic digestion model in laboratory and pilot-scale conditions. *IFAC Proceedings Volumes*, 44(1), 6224–6229.

Tapia-Venegas, E., Ramirez, J.E., Donoso-Brauo, A., Jorquera, L., Steyer, J.P., and Ruiz-Filippi, G. (2013). Biohydrogen production during acidogenic fermentation in a multistage stirred tank reactor. *International Journal of Hydrogen Energy*, 38(5), 2185–2190.

Wang, H., Kalchev, B., Yang, T., Simeonov, I., and Christov, N. (2014). Modelling and composed recursive model free control for the anaerobic digestion process. *China Sciencepaper*, 187, 265–278.

Wang, H., Tian, Y., Kalchev, B., Simeonov, I., and Christov, N. (2013). Pilot anaerobic plant's description, modeling and output feedback control. *IEEE*.

Xing, W. and Zhao, Y.C. (2009). A bench scale study of fermentative hydrogen and methane production from food waste in integrated two-stage process. *International Journal of Hydrogen Energy*, 34(1), 245–254.